Vítor Monteiro, J. G. Pinto, Mohamed Tanta, Bruno Exposto, J. C. Aparício Fernandes, João L. Afonso

"Comprehensive Analysis and Cost Estimation of Five-Level Bidirectional Converters For Electric Vehicles Operation in Smart Cities Context"

COMPREHENSIVE ANALYSIS AND COST ESTIMATION OF FIVE-LEVEL BIDIRECTIONAL CONVERTERS FOR ELECTRIC VEHICLES OPERATION IN SMART CITIES CONTEXT

Vítor Monteiro[*], J. G. Pinto, Mohamed Tanta, Bruno Exposto, J. C. Aparício Fernandes, João L. Afonso

Centro ALGORITMI – University of Minho, Guimarães – Portugal

* Corresponding author: vitor.monteiro@algoritmi.uminho.pt, University of Minho, Campus de Azurém, 4800-058 Guimarães, Portugal

KEYWORDS

Energy Efficiency; Power Converters; Smart Grids

ABSTRACT

A comprehensive analysis, comparison and cost estimation of five-level bidirectional converters for the electric vehicle (EV) operation in smart cities context is presented in this paper. Nowadays, five-level converters are widely used with success to interface between the power grid and renewable energy sources, as well as, to operate as motor drivers. Therefore, with the EV introduction into the power grids arises a new opportunity to use such five-level converters as interface between the power grid and the EV batteries, i.e., in on-board charger applications. Moreover, considering the future scenarios of smart grids and smart cities, the five-level bidirectional converters will be essential for the operation modes grid-to-vehicle (G2V, charging the batteries from the power grid) and vehicle-to-grid (V2G, returning energy from the batteries to the power grid). In this context, this paper presents an aggregation of the most important five-level bidirectional converter topologies that can be applied for on-board EV chargers in smart cities context. Along the paper it is presented a detailed description of the hardware and control algorithms of the five-level converters, and are also presented and explained simulation results performed under realistic operating conditions. Finally, it is presented the cost estimation for a real application considering the hardware requirements for each one of the converters.

INTRODUCTION

Nowadays, plug-in electric vehicles (EVs) are emerging as the main supporter for the electric mobility in smart cities (Rajashekara, 2013)(Milberg, 2011). The battery charging is guaranteed by a slow battery charging process through on-board chargers or by a fast battery charging process through off-board chargers (Monteiro, 2015)(Monteiro, 2016). In this context, a comprehensive analysis and a cost estimation for five-level bidirectional converters that can be used in the on-board EV chargers are presented, focusing their operation properties in smart grids context. With the introduction of EVs in smart grids will emerge a diversity of advantages towards energy efficiency and power quality improvement (Inoa, 2011). In smart grids scenario, EVs will be able to perform the battery charging process from the power grid, denominated as a grid-to-vehicle (G2V) operation mode, or by using bidirectional battery chargers, they can be controlled to deliver energy back to the power grid, denominated as a vehicle-to-grid (V2G) operation mode (Pinto, 2013). By controlling these operation modes, EVs can represent a very important asset to the power grid, allowing to define advantageous schedules of operation with different power levels, considering the four quadrants operation (Kisacikoglu, 2010)(Monteiro, 2016). The on-board EVs battery chargers should operate with a sinusoidal grid current in phase with the power grid voltage in order to prevent power quality problems, mainly the problems associated with the total harmonic distortion and the power factor. Typically, EV battery chargers are designed with two or three-level ac-dc converters (Wong, 2012)(Monteiro, 2016), however, by increasing the number of voltage levels of the converter, it is possible to reduce the size of the passive filters used in the connection to the power grid. Nevertheless, the number of voltage levels cannot be increased indefinitely (i.e., much higher than five-levels) due to the high power density that is required for on-board EV chargers. In the literature it can be found several five-level topologies for different purposes. A five-level active rectifier for high-speed generator applications is presented in (Grbovic, 2016). A five-level unidirectional active rectifier for power factor correction converters is proposed and experimentally verified in (Monteiro, 2015). Similarly, an improved five-level bidirectional converter operating as an active rectifier and as a grid tie inverter is proposed and experimentally verified in (Monteiro, 2016). A modular five-level unidirectional converter operating as a grid tie inverter for renewable applications is presented in (Elsheikh, 2011). A new five-level converter also operating as a grid tie inverter for renewables applications is presented in (Loukriz, 2015), and an active neutral-point clamped five-level converter for motor driver applications is presented in (Wang, 2015). Although these

five-level converters have been validated for several applications, a great part of them was never validated in on-board EV chargers, neither was established a comparison between them. In this context, the main contributions of this paper are: aggregation in a single paper of the most important five-level bidirectional converters that can be applicable for on-board EV chargers in smart grids context; comparative cost analysis in terms of hardware implementation and in terms of operation in smart grids context. Section II presents a detailed description about the hardware and the control algorithms of the converters under comparison. Section III presents the main simulation results for different operation scenarios framed with smart cities and smart grids. Section IV presents the cost analysis comparison in terms of the converters development. Finally, Section VI presents the main conclusions that can be retrieved.

DESCRIPTION AND CONTROL ALGORITHMS

This section presents the description and the control algorithms of the different five-level bidirectional converters for EV battery chargers under comparison in this paper.

Description of the Converters

Figure 1 presents the four five-level bidirectional converters for EV battery chargers under comparison in this paper. Taking into account a real application were considered IGBTs in all the converters and an inductor as a passive filter to connect the converters with the power grid. The converter presented in Figure 1(a) is composed by a full-bridge full-controlled h-bridge and by a bidirectional bipolar cell, composed by two IGBTs with a common emitter configuration, which is connected between the middle point of one leg of the h-bridge and the middle point of the dc-link. The converter presented in Figure 1(b) is composed by a full-bridge full-controlled h-bridge and by a bidirectional bipolar cell, composed by two IGBTs and two diodes. This cell is also connected between the middle point of one leg of the h-bridge and the middle point of the dc-link. The converter presented in Figure 1(c) is also composed by a full-bridge full-controlled h-bridge and by four bidirectional and bipolar cells, composed by two IGBTs with a common emitter configuration, two of them are connected between the phase wire and the middle point of the dc-link, and the other two cells are connected between the neutral wire and the middle point of the dc-link. The converter presented in Figure 1(d) is composed by two full-bridge full-controlled h-bridges with a cascade configuration, i.e., the middle point of one leg of the h-bridge is connected to the middle point of the other h-bridge. It is important to note that this converter has two independent output dc-links. This can be an advantage or a disadvantage depending of the dc-dc converter used to interface to the batteries.
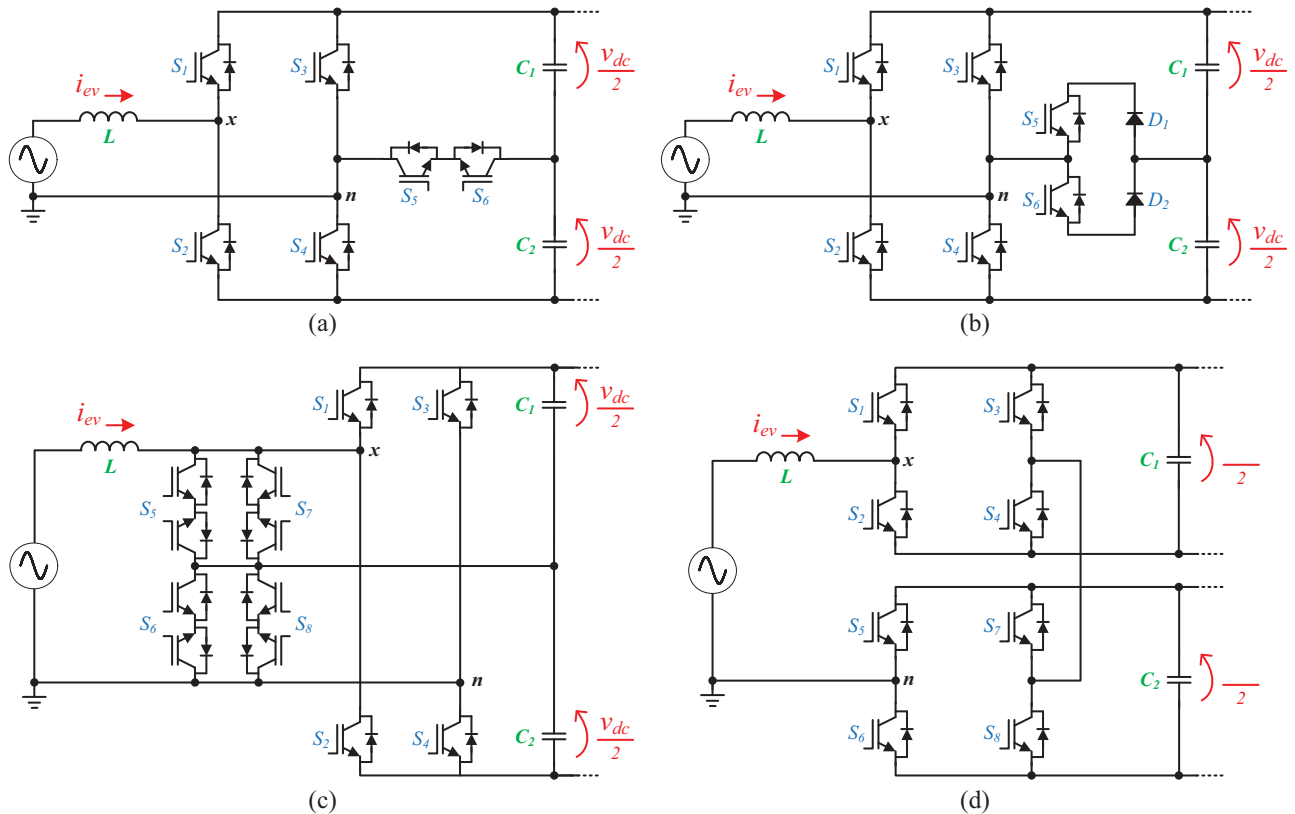

Figure 1: Five-level bidirectional converter topologies under comparison for EV battery chargers.

Control Algorithm Description

This item presents a detailed description about the digital control algorithm used to control the five-level bidirectional converters under comparison. Taking into account the boost-type nature of the converters, the output voltage (v_{dc}) should be greater than the maximum voltage of the power grid (i.e., the input voltage). Therefore, a proportional-integral (PI) controller is used to control the dc-link voltage according to the reference established. In the scope of this paper was considered a power grid voltage with a nominal root mean square (rms) value of 230 V and a dc-link voltage of 400 V. The output of the PI controller is added to the nominal power in the dc-side (multiplication of v_{bat} with i_{bat}, which represents the power to charge the battery), where it can be connected directly to the EV batteries or to a dc-dc converter. The resultant power is divided by the square value of the power grid rms voltage (V_G). Then, the output value is multiplied by the square root of the output signal obtained from a phase-locked loop (PLL), and by the rms value of the power grid voltage in order to obtain the EV grid current reference ($i_{ev}{}^*$). It is important to note that the PLL is used in order to obtain a sinusoidal grid current reference even with a distorted power grid voltage, i.e., with such strategy, the EV will consume a sinusoidal current contributing to preserve the power quality in the electrical installation where it is plugged-in. The output of the PLL is a sinusoidal signal with unitary amplitude. Therefore, it is necessary to multiply such signal by the rms value in order to obtain an output signal that is proportional to the fundamental power grid voltage component. This algorithm is shown in Figure 2(a) and it is used to establish the EV grid current reference. It is identified in this paper as a current reference theory. The EV grid current reference ($i_{ev}{}^*$) is used in a predictive current control to define the voltage that each convert must produce in order to obtain a sinusoidal EV grid current (i_{ev}). This current control strategy uses the actual [k] and previous values [k-1] values of the current reference ($i_{ev}{}^*$) and the produced current (i_{ev}). The error between two times the actual value of the EV current reference ($i_{ev}*[k]$) and the actual value of the EV current ($i_{ev}[k]$) is subtracted the previous value of the EV current reference ($i_{ev}*[k$-1]). To the resultant value is subtracted the error in the previous sampling, i.e., the error between the previous EV current reference ($i_{ev}*[k$-1]) and the previous EV current ($i_{ev}[k]$). The output value is then multiplied by the value of the coupling filter inductor (L) and by the value of the sampling frequency (f_s). The resultant value is then subtracted to the actual value of the power grid voltage ($v_g[k]$) in order to obtain the voltage reference ($v_{conv}*$) that the converter must produce to control the EV grid current (i_{ev}). This algorithm is shown in Figure 2(b) and it is used to establish the voltage produced by the converter. This control is identified in this paper as current control theory.
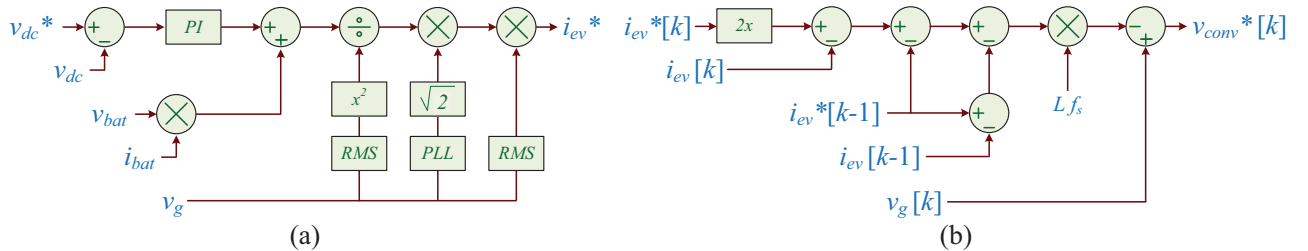

Figure 2: Control algorithm: (a) Current reference theory; (b) Current control theory.

SIMULATION RESULTS

This section presents the main simulation results for the four five-level converter topologies under comparison. These results were obtained during the operation as an active rectifier (i.e., charging the batteries from the power grid through the G2V operation mode) and during the operation as a grid-tie inverter (i.e., discharging the batteries to the power grid through the V2G operation mode). The results were obtained in transient and steady state. The converters were simulated with the same conditions of operation and by considering the parameters presented in the Table 1.

Table 1: Parameters used in the Simulation Model.

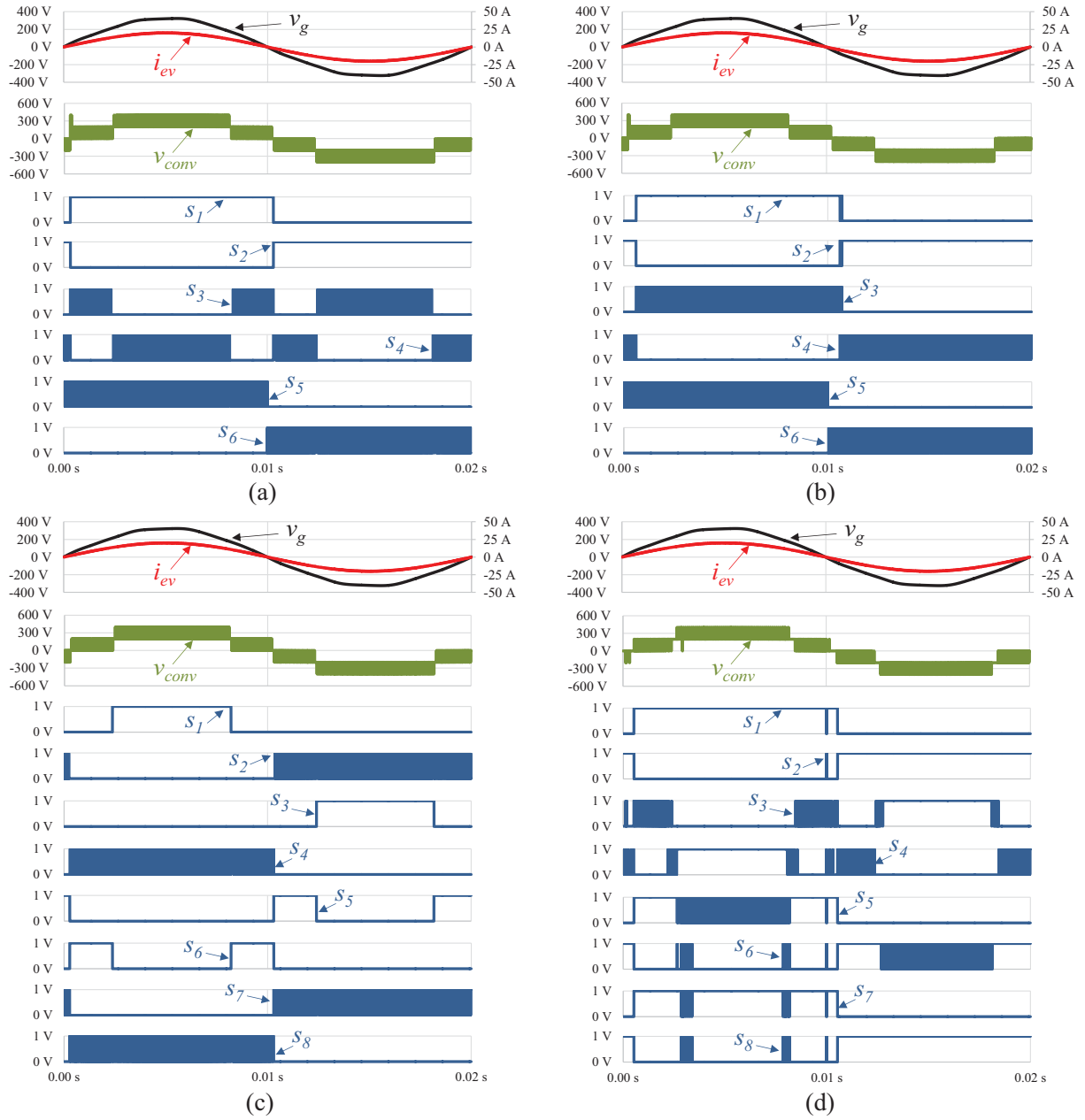| Parameter	Value	Unit
Power Grid Voltage	230	V
Power Grid Frequency	50	Hz
Maximum Current Reference	20	A
Dc-link Voltage	400	V
Total Harmonic Distortion @ Full Power	< 5%	–
Power Factor @ Full Power	> 0.99	–
Sampling Frequency	40	kHz
Switching Frequency	20	kHz
Coupling Inductor	5	mH

Figure 3: Simulation results of the four five-level bidirectional converter topologies under comparison: Power grid voltage (v_g); EV grid current (i_{ev}); Voltage produced by the converter (v_{conv}); IGBTs control signals ($s_1...s_8$).

Figure 3 shows some simulation results of the power grid voltage (v_g), the EV grid current (i_{ev}), the voltage produced by the converter (v_{conv}), and the IGBTs control signals ($s_1...s_8$). For the converter presented in Figure 1(a), and as expected, the EV grid current (i_{ev}) is sinusoidal and in phase with the power grid voltage (v_g), and the voltage produced by the converter can assume five distinct voltage levels. The IGBTs s_1 and s_2 are switched at the frequency of the power grid voltage (i.e., 50 Hz), the IGBT s_5 is only switched during the positive half-cycle and the IGBT s_6 is only switched during the negative half-cycle. During the positive half-cycle, the IGBT s_3 is switched when the voltage produced varies between 0 and $v_{dc}/2$ and the IGBT s_4 is switched when the voltage produced varies between $v_{dc}/2$ and v_{dc}. During the negative half-cycle, the IGBT s_3 is switched when the voltage produced varies between $-v_{dc}/2$ and $-v_{dc}$ and the IGBT s_4 is switched when the voltage produced varies between 0 and $-v_{dc}/2$. Figure 3(a) shows the simulation results obtained for this converter. For the converter presented in Figure 1(b), and similarly to the previous case, the EV grid current (i_{ev}) is sinusoidal and in phase with the power grid voltage (v_g), and the voltage produced by the converter can assume five distinct voltage levels. The IGBTs s_1, s_2, s_5 and s_6 are switched as described for the previous converter. On the other hand, the IGBT s_3 is switched during all the positive half-cycle and the IGBT s_4 is switched during all the negative half-cycle. Figure 3(b) shows the simulation results obtained for this converter. For the converter presented in Figure 1(c), and as expected, the EV grid current (i_{ev}) is sinusoidal and in phase with the power grid voltage (v_g), and the

voltage produced by the converter can assume five distinct voltage levels. The IGBTs s_1 is only on when the voltage produced varies between $v_{dc}/2$ and v_{dc}, and the IGBTs s_3 is only on when the voltage produced varies between -$v_{dc}/2$ and $-v_{dc}$. The IGBT s_2 is switched during all the negative half-cycle and the IGBT s_4 is switched during all the positive half-cycle. The IGBT s_5 is only switched when the voltage produced varies between 0 and $-v_{dc}/2$, and the IGBT s_6 is only switched when the voltage produced varies between 0 and $v_{dc}/2$. The IGBT s_7 is switched during all the negative half-cycle and the IGBT s_8 is switched during all the positive half-cycle. Figure 3(c) shows the simulation results obtained for this converter. For the converter presented in Figure 1(d), and as expected, the EV grid current (i_{ev}) is sinusoidal and in phase with the power grid voltage (v_g), and the voltage produced by the converter can assume five distinct voltage levels. The IGBTs s_1 is always on during the positive half-cycle and the IGBT s_2 is always on during the negative half-cycle. The IGBT s_3 is switched when the voltage produced varies between 0 and $v_{dc}/2$ and is ON when the voltage produced varies between $-v_{dc}/2$ and $-v_{dc}$. On the other hand, the IGBT s_4 is switched when the voltage produced varies between 0 and -$v_{dc}/2$ and is ON when the voltage produced varies between $v_{dc}/2$ and v_{dc}. The IGBT s_5 is switched when the voltage produced varies between $v_{dc}/2$ and v_{dc} and is ON when the voltage produced varies between 0 and $v_{dc}/2$. On the other hand, the IGBT s_6 is switched when the voltage produced varies between -$v_{dc}/2$ and -v_{dc} and is ON when the voltage produced varies between 0 and -$v_{dc}/2$. The IGBT s_7 is ON during the positive half-cycle and the IGBT s_8 is ON during the negative half-cycle. Figure 3(d) shows the simulation results obtained for this converter.

Figure 4 shows the power grid voltage (v_g) and the EV grid current (i_{ev}) during the G2V and V2G operation modes. This simulation result was obtained to show that the EV grid current is sinusoidal during both operation modes and is in phase (G2V) or phase opposition (V2G) with the power grid voltage. It is important to note that were simulated all the converters under comparison, however, the obtained EV grid current is equal for all the converters. Therefore, it is not relevant repeat the same result for all the converter.
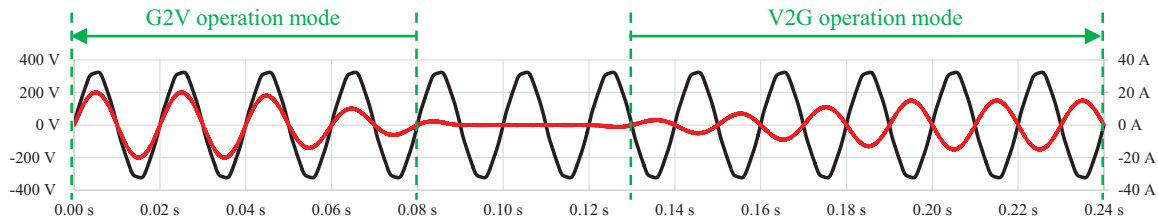

Figure 4: Simulation results during the G2V and V2G operation modes.

COST ANALYSIS COMPARISON

In this section is presented a brief cost analysis comparison. In such comparison were only considered the direct costs associated with the hardware. Figure 5(a) shows the number of independently outputs, the number of IGBTs modules used in the legs (modules with two IGBTs, i.e., with the emitter of the top IGBT connected to the collector of the bottom IGBT), the number of IGBTs modules used in the bidirectional cells (modules with two IGBTs, i.e., with the collector of the top IGBT connected to the collector of the bottom IGBT), and the number of driver boards (where, each driver board is used to control each IGBTs modules). It is important to note that all the converters have the same number of voltage and current sensors, the same number of digital control platforms (including the microcontroller and signal conditioning circuits), and the same number of passive filters (i.e., the coupling inductor with the power grid and the output dc-link capacitors). Therefore, these items were not considered in this comparison. Figure 5(b) shows the total cost estimation for the development of the aforementioned converters, and the individual cost of the aforementioned IGBTs modules and drivers boards. It is important to note that these costs were determined based on commercial costs for power electronic devices (Semikron, 2017). As it can be seen, based on such online prices, the converter presented in Figure 1(c) is the more expensive and the converter presented in Figure 1(a) is the cheaper.

CONCLUSIONS

This paper presents a comprehensive analysis, comparison and cost estimation of five-level bidirectional converters for on-board electric vehicles (EV) chargers considering their operation in smart cities, which are the main contributions of the paper. Five-level bidirectional converters are used for several applications, and consequently, with the EV introduction into the power grids, arises a new opportunity to use such converters to interface between the power grid and the EV batteries. converters under comparison were validated through computer simulations under realistic operating conditions, and considering the EV charging from the power grid (G2V - grid-to-vehicle mode) and the EV discharging to the power grid (V2G - vehicle-to-grid mode). As presented in the obtained results for all the converters, the grid current is sinusoidal and in phase (G2V mode) or in phase opposition (V2G mode) with the power grid voltage, and as expected, the voltage produced by each converter can assume five distinct levels. Along the paper are presented in detail the hardware description (the number and type of devices used) and the control algorithms (current reference theory and current control theory), and it is established a cost estimation based on the requirements of each converter.

The cost estimation of each converter is based on commercial costs for power electronic devices, and is useful to identify the more expensive and the cheaper five-level bidirectional converter for on-board EV battery chargers.
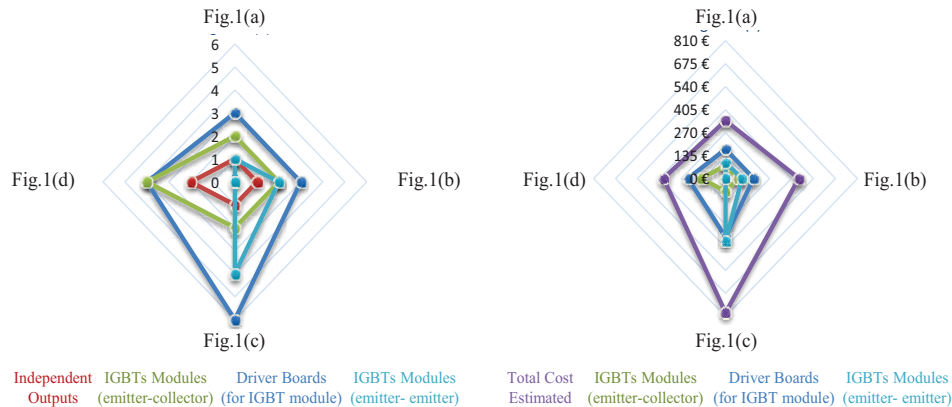

Figure 5: Comparison of the five-level bidirectional converters presented in Figure 1 in terms of:
(a) Number of devices used; (b) Cost of the main devices and total cost estimation.

ACKNOWLEDGMENTS

REFERENCES

Elsheikh, M. G., Ahmed, M. E., Abdelkarem, E., Orabi, M., (2011). Single-Phase Five-Level Inverter with Less Number of Power Elements. IEEE INTELEC International Telecommunications Energy Conference.

Grbovic, P., Lidozzi, A., Solero, L., Crescimbini, F., (2016). Five-Level Unidirectional T-Rectifier for High Speed Gen-Set Applications. IEEE Transactions on Industrial Applications.

Inoa, E., Wang, J., (2011). PHEV Charging Strategies for Maximized Energy Saving. IEEE Transactions on Vehicular Technology.

Kisacikoglu, M. C., Ozpineci, B., Tolbert, L. M., (2010). Examination of a PHEV Bidirectional Charger System for V2G Reactive Power Compensation. IEEE APEC Applied Power Electronics Conference and Exposition.

Loukriz, A. H., Dudley, S., Quinlan, T., Walker, S. D., (2016). Experimental Realization of a Single-Phase Five Level Inverter for PV Applications. IEEE COMPEL Control and Modeling for Power Electronics.

Milberg, J., Schlenker, A., (2011). Plug into the Future. IEEE Power Energy Magazine.

Monteiro, V., Carmo, J. P., Pinto, J. G., Afonso, J. L., (2016). A Flexible Infrastructure for Dynamic Power Control of Electric Vehicle Battery Chargers. IEEE Transactions on Vehicular Technology.

Monteiro, V., Ferreira, J. C., Meléndez, A. A. N., Afonso, J. L., (2013). Electric Vehicles On-Board Battery Charger for the Future Smart Grids. In Technological Innovation for the Internet of Things. L. M. Camarinha-Matos, S. Tomic, P. Graça, Ed. Springer.

Monteiro, V., Ferreira, J. C., Meléndez, A. A. N., Afonso, J. L., (2016). Model Predictive Control Applied to an Improved Five-Level Bidirectional Converter. IEEE Transactions Industrial Electronics.

Monteiro, V., Pinto, J. G., Exposto, B., Afonso, J. L., (2015). Comprehensive Comparison of a Current-Source and a Voltage-Source Converter for Three-Phase EV Fast Battery Chargers. CPE International Conference on Compatibility and Power Electronics.

Monteiro, V., Meléndez, A. A. N., Ferreira, J. C., Couto, C., Afonso, J. L., (2015). Experimental Validation of a Proposed Single-Phase Five-Level Active Rectifier Operating with Model Predictive Current Control. IEEE Industrial Electronics Conference.

Monteiro, V., Pinto, J. G., Afonso, J. L., (2016). Operation Modes for the Electric Vehicle in Smart Grids and Smart Homes: Present and Proposed Modes. Transactions on Vehicular Technology.

Monteiro, V., Exposto, B., Ferreira, J. C., Afonso, J. L., (2016). Improved Vehicle-to-Home (iV2H) Operation Mode: Experimental Analysis of the Electric Vehicle as Off-Line UPS. IEEE Trans. Smart Grid.

Monteiro, V., Ferreira, J. C., Pedrosa, D., Sepúlveda, M. J., Aparício Fernandes, J. C., Afonso, J. L., (2016). Comprehensive Analysis and Comparison of Digital Current Control Techniques for Active Rectifiers. CONTROLO 2016 Portuguese Conference on Automatic Control.

Rajashekara, K., (2013). Present Status and Future Trends in Electric Vehicle Propulsion Technologies. IEEE Journal of Emerging and Selected Topics in Power Electronics.

"SEMIKRON – innovation+service". Available online (14 march 2017). http://shop.semikron.com/

Wang, K., Xu, L., Zheng, Z., Li, Y., (2015). Capacitor Voltage Balancing of a Five-Level ANPC Converter Using Phase-Shifted PWM. IEEE Trans. Power Electronics.

Wong, N., Kazerani, M., (2012). A Review of Bidirectional On-Board Charger Topologies for Plug-In Vehicles. IEEE CCECE Canadian Conference on Electrical & Computer Engineering.